Experimental Validation of a Closed-Loop Respiratory Control Model using Dynamic Clamp

Casey O. Diekman[1], Peter J. Thomas[2], and Christopher G. Wilson[3]

Abstract— **We have previously introduced a model for closed-loop respiratory control incorporating an explicit conductance-based model of bursting pacemaker cells driven by hypoxia sensitive chemosensory feedback. Numerical solution of the model equations revealed two qualitatively distinct asymptotically stable dynamical behaviors: one analogous to regular breathing (eupnea), and a second analogous to pathologically rapid, shallow breathing (tachypnea). As an experimental test of this model, we created a hybrid *in vitro/in silico* circuit. We used Real Time eXperimental Interface (RTXI) dynamic clamp to incorporate a living pacemaker cell recorded *in vitro* into a numerical simulation of the closed-loop control model in real time. Here we show that the hybrid circuit can sustain the same bistable behavior as the purely computational model, and we assess the ability of the hybrid circuit to recover from simulated bouts of transient hypoxia.**

I. INTRODUCTION

In [3], [4] Butera, Rinzel and Smith (BRS) introduced a model for autorhythmic activity in neurons of the preBötzinger Complex (pBC), a brainstem center that is essential for normal breathing [17]. The BRS model accounts for many observed properties of autorhythmic pBC cells, including the existence of three dynamical regimes: quiescence in response to low drive conditions, regular bursting in response to moderate drive conditions, and rapid steady beating in response to elevated drive conditions. As part of a respiratory control system, both the quiescent and beating states would fail to drive lung activity and gas exchange adequately to maintain appropriate levels of blood O_2. In [7], we incorporated the BRS equations into a closed-loop respiratory control model, and confirmed the existence of two qualitatively distinct asymptotically stable behaviors, corresponding to bursting and beating. When subject to sustained hypoxia, increased chemosensory input drove the model neuron to the pathological state of sustained beating. We also demonstrated that the BRS model possesses a previously unreported capacity for *autoresuscitation*: when hypoxia is first imposed, through a rapid reduction of blood O_2, the BRS model responds with a transient barrage of activity which can force an abnormally large expansion of the lung, temporarily increasing gas exchange and potentially restoring blood O_2. We observed that the BRS system could "survive" the imposition of hypoxia for various combinations of duration and severity of reduced blood O_2 [7].

Computational models are often used to provide insight into the behavior of biological systems. In most instances these insights are "postdictive" rather than predictive [1]. A strong test of a biological model is whether it can predict aspects of the behavior of a biological system, which can be subsequently tested [13]. Here we report on dynamic clamp experiments in which we tested the closed-loop control model of [7] by implementing a hybrid *in vitro/in silico* circuit, in which a living cell from a pBC slice preparation replaced the model's BRS-based central pattern generator (CPG).

II. METHODS

Dynamic clamp systems [16] such as RTXI [10] can record voltage from a cell and supply artificial conductances in the form of current injection adjusted in real time based on the cell's voltage. Within RTXI, we constructed a modular representation of the control circuit from [7] as shown in Fig. 1A.

A. Hybrid circuit

We patched onto cells in the pBC, and used the recorded membrane potential (V) as input to a module representing the respiratory musculature. This module includes synaptic activation of a motor unit (α) that causes changes in lung volume (vol). Air intake during lung expansions increases the partial pressure of oxygen in the lung ($PO2_{lung}$). The partial pressure of oxygen in the blood ($PO2_{blood}$) increases due to oxygen transfer from the lungs, and decreases due to metabolic demand. The equations for these model components are given in the Appendix. A fuller description of our modeling rationale can be found in [6].

Following [7], we model the hypoxia chemosensation pathway with a sigmoidal relationship between $PO2_{blood}$ (mmHg), that determines g_{tonic} (nS), a conductance representing external drive to the pBC. We assume that increasing oxygen deficiency increases the respiratory drive:

$$g_{tonic} = 0.5\left(1 - \tanh\left(\frac{PO2_{blood} - 100}{30}\right)\right) \qquad (1)$$

[1]C. O. Diekman is with the Department of Mathematical Sciences and the Institute for Brain and Neuroscience Research, New Jersey Institute of Technology, Newark, NJ 07102, USA diekman at njit.edu

[2]P. J. Thomas is with the Department of Mathematics, Applied Mathematics, and Statistics, Department of Biology, Department of Cognitive Science, and Department of Electrical Engineering and Computer Science, Case Western Reserve University, Cleveland, OH 44106, USA pjt9 at case.edu

[3]C. G. Wilson is with the Center for Perinatal Biology, Division of Physiology, School of Medicine, Loma Linda University, Loma Linda, CA 92350, USA cgwilson at llu.edu

This work was supported in part by NSF grants DMS-1413770 and DEB-1654989 to PJT and DMS-1555237 to COD, NIH grants HL-62527 and HL-81622 to CGW, and the Mathematical Biosciences Institute under NSF grant DMS-1440386.

978-1-5386-3646-6/18/$31.00 ©2018 IEEE

The computed external conductance is then applied to the patch-clamped pBC cell. The amount of current injected (I_{tonic}, pA) also depends on the cell's membrane potential:

$$I_{\text{tonic}} = g_{\text{tonic}}(V - E_{\text{syn}}) \tag{2}$$

where $E_{\text{syn}} = 0$ mV.

After patching onto a bursting pBC cell, we isolated the cell from excitatory synaptic inputs by applying CNQX (6-cyano-7-nitroquinoxaline-2,3-dione) to block AMPA and kainate receptors. If after application of CNQX the cell was no longer bursting, we injected a simulated BRS persistent sodium current (I_{NaP}, pA) through RTXI, in order to recover bursting before performing closed-loop or autoresuscitation experiments:

$$I_{\text{NaP}} = g_{\text{NaP}} p_\infty h (V - E_{\text{NaP}}) \tag{3}$$

$$\frac{dh}{dt} = \frac{h_\infty - h}{\tau_h} \tag{4}$$

$$x_\infty = \{1 + \exp[(V - \theta_x)/\sigma_x]\}^{-1} \tag{5}$$

$$\tau_x = \bar{\tau}_x / \cosh[(V - \theta_x)/(2\sigma_x)] \tag{6}$$

for gating variable $x \in \{p, h\}$ where $\theta_p = 40$ mV, $\sigma_p = -6, \theta_h = -48, \sigma_h = 6, \bar{\tau}_h = 10{,}000$ ms, and $E_{\text{NaP}} = 50$ mV. Butera and colleagues demonstrated that a persistent (i.e. slowly inactivating) sodium conductance [8], [12] was necessary and sufficient to generate bursting in a model consistent with the properties of spontaneous burst activity of autorhythmic neurons recorded in organotypic slice preparations from neonatal rats [3], [5]. However, due to natural biological variability, individual cells have different amounts of endogenous NaP conductance [12], [18]. By incorporating a baseline level of simulated NaP conductance into our hybrid circuit, we raised the cell's endogenous NaP conductance to a level sufficient to kindle bursting activity.

B. Computational circuit

In order to compare the behavior of the hybrid circuit with a purely computational implementation, we performed simulations in which the patched-clamped pBC cell was replaced by a BRS model cell. In the purely computational model, the membrane potential (V) is given by:

$$C\frac{dV}{dt} = I_{\text{app}} - I_{\text{NaP}} - I_{\text{Na}} - I_{\text{K}} - I_{\text{L}} - I_{\text{tonic}} \tag{7}$$

$$I_{\text{Na}} = g_{\text{Na}} m_\infty^3 (1 - n)(V - E_{\text{Na}}) \tag{8}$$

$$I_{\text{K}} = g_{\text{K}} n^4 (V - E_{\text{K}}) \tag{9}$$

$$I_{\text{L}} = g_{\text{L}} (V - E_{\text{L}}) \tag{10}$$

$$\frac{dn}{dt} = \frac{n_\infty - n}{\tau_n} \tag{11}$$

where $C = 21$ pF, $I_{\text{app}} = 0$ pA, $\theta_m = -34$ mV, $\sigma_m = -5, \theta_n = -29, \sigma_n = -4, \bar{\tau}_n = 10$ ms, $g_{\text{Na}} = 28$ nS, $g_{\text{K}} = 11.2, g_{\text{L}} = 2.8, E_{\text{Na}} = 50$ mV, $E_{\text{K}} = -85, E_{\text{L}} = -65$. I_{NaP} is as given in (3), with $g_{\text{NaP}} = 2.8$ nS.

Naturally occurring populations of neurons show significant individual variability within cell types [12], [14]. After running the hybrid respiratory control loop protocol with a particular pBC cell included *via* dynamic clamp, we adjusted the standard BRS parameters to improve the correspondence between model behavior and the hybrid circuit. First, we set C to the measured cell capacitance, and set the reversal potentials within the BRS model to match potentials based on the recording solutions used in the experiments ($E_{\text{Na}} = 65$ mV, $E_K = -72$ mV). In some cases, even with these adjustments, the modified BRS model showed spontaneous bursting on a time scale $2-4\times$ faster than the cell recorded in open-loop conditions. We found that adding a *truly* persistent (i.e. non-inactivating [19]) sodium current ($I_{\text{Na(NI)}}$) led to spontaneous bursting on a time scale matching that of the patched cell:

$$I_{\text{Na(NI)}} = g_{\text{Na(NI)}} p_\infty (V - E_{\text{Na}}) \tag{12}$$

Model simulations and analysis were performed using RTXI, XPPAUT, and MATLAB.

C. Animal experiments and electrophysiology

All procedures were performed in accordance with protocols approved by the Case Western Reserve University Institutional Animal Care and Use Committee. Brainstem slices from Sprague-Dawley rats were prepared as described in [6]. Intracellular signals were recorded with a HEKA EPC-10D amplier (HEKA Elektronik GmbH, Germany) controlled by Real-Time eXperiment Interface software (http://www.rtxi.org) running at a cycle frequency of 10 kHz.

III. Results

A. Bistability in the hybrid circuit

The bistability of eupnea-like and tachypnea-like breathing observed in the closed-loop model of [7] depends on properties of the BRS model of pBC cells. We verified that, as expected, pBC cells themselves possess these properties and can sustain two distinct stable behaviors within the closed-loop control system, by using an *in vitro* brainstem slice preparation containing the pBC, premotor neurons and the hypoglossal nerve (XIIn) rootlet. We created hybrid circuits by patching on to inspiratory pBC cells (cells that fired in phase with the XIIn rhythm), and used the recorded membrane potential to drive the muscle and gas exchange compartments of the model in real time. We closed the control loop *via* dynamic clamp; the simulated $PO2_{\text{blood}}$ level determined g_{tonic}, which, along with the measured membrane potential, was used to compute the amount of current (I_{tonic}) to inject into the cell, as diagrammed in Fig. 1A.

The hybrid circuit exhibited two distinct regimes. In one regime, the cell was bursting (Fig. 1B left column), which led to simulated lung expansions that were sufficient to maintain $PO2_{\text{blood}}$ above 100 mmHg in the model, thus keeping g_{tonic} below 0.5 nS. In the second regime, the cell was not bursting, but instead firing tonically (Fig. 1B right column). The beating-like activity drove simulated lung expansions that were too small to sustain effective gas exchange. In this regime, $PO2_{\text{blood}}$ remained low (around 60 mmHg) in the model, leading to high drive ($g_{\text{tonic}} \approx 1$ nS) that reinforced the beating behavior. These data confirm that inspiratory cells

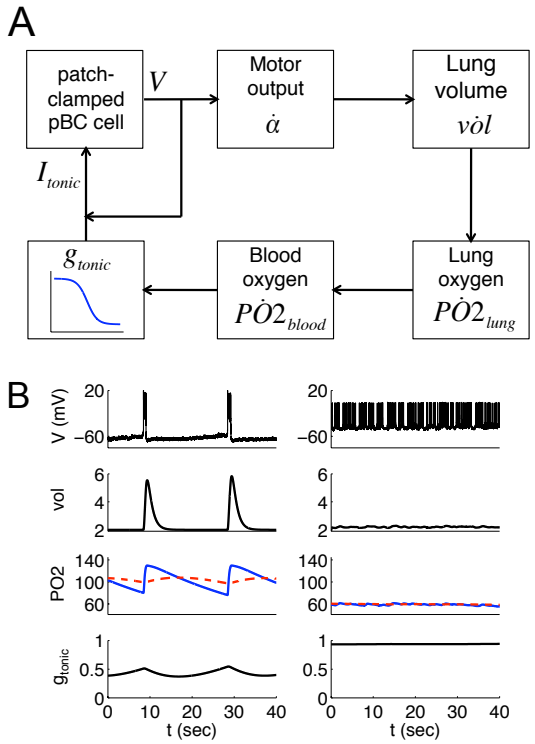

Fig. 1. Bistability in a hybrid *in vitro/in silico* respiratory control loop. (**A**) Schematic showing modular construction of the control loop. Motor output, lung volume, lung oxygen, blood oxygen and g_{tonic} modules were implemented within RTXI. Through RTXI's dynamic clamp, we injected artificial conductances (g_{tonic} and supplemental g_{NaP}, see Methods) to a patch-clamped pBC cell *in vitro*, and used the cell's membrane voltage as input to the motor module in real time. (**B**) Left column: stable eupnea-like, fictive breathing activity in the closed-loop hybrid circuit. V (top trace) is the voltage recorded from the *in vitro* cell; the other variables (vol (L), second trace; PO2_{lung} (mmHg), blue trace, $\text{PO2}_{\text{blood}}$ (mmHg), red trace, g_{tonic} (nS), bottom trace) were computed in real time within RTXI. Right column: stable tachypnea-like activity in the hybrid circuit. Note the small deflections of lung volume; depression of PO2 (both blood and lung) near 60 mmHg, and the elevation of g_{tonic}.

taken from a pBC network *in vitro* show the same type of bistability predicted by our purely computational control loop [7].

B. Autoresuscitation in the hybrid circuit

The autoresuscitation phenomenon observed in the purely computational control loop [7] also depends on recently discovered properties of the BRS model, in particular, its transient response to rapid imposition of simulated hypoxia. We tested autoresuscitation in the hybrid circuit by temporarily clamping simulated $\text{PO2}_{\text{blood}}$ at 60 mmHg to represent the imposition of hypoxia. As shown in Fig. 2A, if the clamp was short enough in duration ($\tau \leq 50$ seconds), then $\text{PO2}_{\text{blood}}$ was able to recover to eupneic values after the clamp was released. In these cases the cell was able to escape the basin of attraction of tachypnea. When the clamp was held for longer ($\tau = 60$ seconds), the cell could not escape the beating state and $\text{PO2}_{\text{blood}}$ did not recover after the clamp was released. Thus, the pBC cells showed autoresuscitation qualitatively consistent with predictions based on the BRS model cell behavior.

However, the time course of autoresuscitation in the hybrid circuit was quantitatively different from that predicted by the purely computational control loop incorporating the standard BRS model neuron. Whereas the hybrid circuit with an actual pBC cell recovered to eupnea after clamps as long as 50 seconds, the purely computational circuit with the BRS equations replacing the pBC cell descended into tachypnea after a clamp of only 700 milliseconds (Fig. 2B). Therefore, after completing the hybrid circuit protocol, we adjusted the parameters of the BRS model to better reproduce the behavior of the hybrid circuit, based on measured parameters of the recorded cell (see Methods, §II-B) as well as the closed-loop data in Fig. 1B. Model cell parameters were chosen so that the recorded and modeled voltage traces had similar burst durations, interburst intervals, numbers of spikes per burst, and within-burst depolarization plateaus. Figure 2C shows the closed-loop behavior of the purely computational circuit after tuning. We then repeated the simulated hypoxia clamp protocol on the tuned purely computational circuit, and found that its behavior more closely matched the autoresuscitation observed in the hybrid circuit (compare Figs. 2A and 2D). The data presented here are from a single recording, however the experiment was repeated on multiple slices and the same qualitative behavior was observed in other cells.

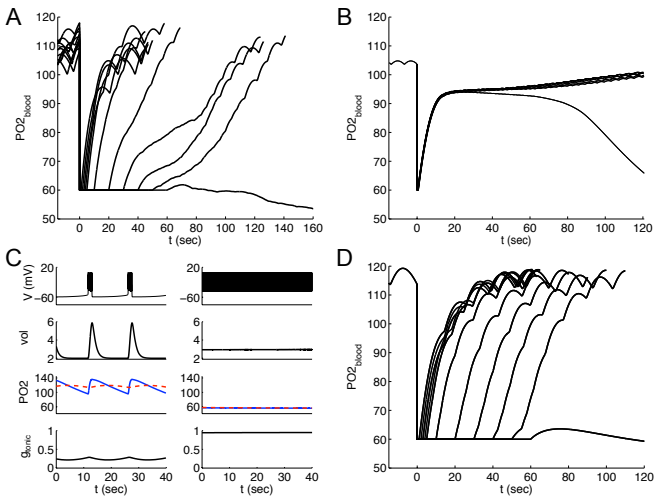

Fig. 2. (**A**) Autoresuscitation in a hybrid circuit, with a biological cell embedded in the closed-loop model. $\text{PO2}_{\text{blood}}$ was clamped to 60 mmHg for τ seconds and then released. For $\tau = 1, 2, 3, 4, 5, 10, 20, 30, 40$ and 50 seconds, $\text{PO2}_{\text{blood}}$ recovered to normal values, and the system returned to eupneic-like fictive breathing. For $\tau = 60$ seconds, $\text{PO2}_{\text{blood}}$ did not return to normal values, and the system exhibited sustained tachypneic-like breathing. (**B**) In a fully computational realization of the hybrid circuit, the biological pBC cell is replaced by the BRS equations with the original parameter values. The computational circuit displays autoresuscitation, but the temporal properties of autoresuscitation do not match the hybrid circuit; the system only recovers to normal $\text{PO2}_{\text{blood}}$ values for clamps of $\tau = 100, 200, 300, 400, 500$ and 600 milliseconds, but does not recover when $\tau = 700$ milliseconds. (**C**) Closed-loop behavior of the purely computational circuit with the parameters of the BRS equations adjusted to match the closed-loop behavior of the hybrid circuit in Fig. 1B. Here, $C = 61$ pF and $g_{\text{Na}} = 50$, $g_{\text{K}} = 20$, $g_{\text{NaP}} = 4$, $g_{\text{Na(NI)}} = 0.22$, $g_{\text{L}} = 4.1$ nS. (**D**) The computational circuit with adjusted BRS parameters more closely reproduces the time course of autoresuscitation observed in the hybrid circuit (**A**).

IV. Discussion

In the respiratory control loop model introduced in [7], bistability of eupnea-like and tachypnea-like behavior, as well as the capacity for autoresuscitation, arise from conductances intrinsic to the respiratory CPG model of Butera, Rinzel and Smith [3]. Here we have demonstrated these behaviors in a hybrid control loop in which the CPG model neuron is replaced by an inspiratory pBC cell in an *in vitro* brainstem slice preparation. Our results also suggest that pBC cells may possess a noninactivating sodium conductance.

Under selective pressure to develop robust control systems, neural networks in the brainstem presumably involve a rich array of currents, neuromodulators, and other homeostatic mechanisms that extend beyond what any one computational model can adequately describe. It is not surprising, therefore, that a single cell participating in an *in vitro* hybrid control circuit led to greater tolerance of simulated hypoxia than that observed in an identical control circuit built around a model cell with nominal parameters selected to exhibit isolated rhythmogenesis. There are many factors that may contribute to even greater robustness in the *in vivo* control circuit. For example, the interactions of multiple cells within a network can stabilize rhythmic activity over a larger dynamic range than a single cell [2], [4], and parametric heterogeneity across a population of coupled oscillators can increase their robustness [9], [15]. Stochastic effects (noise), although not included in the computational model [7], may play an important role as well [20]. It is known that stochastic effects can stabilize or even induce rhythmic activity in respiratory networks [11]. Remarkably, however, in the present case, a model circuit incorporating a single deterministic BRS model neuron proved as robust as a hybrid circuit incorporating an actual pBC cell *in vitro*, upon inclusion of appropriate slow currents. It is striking that the endogenous conductances at the cellular level seem to have a hardwired reflex that may help the organism withstand transient episodes of hypoxia.

APPENDIX

$$\frac{d\alpha}{dt} = r[T](1-\alpha) - r\alpha$$

$$\frac{d}{dt}(vol) = -E_1(vol - Vol_0) + E_2\alpha$$

$$\frac{d}{dt}(PO2_{lung}) = \left(\frac{1}{vol}\right)\left((PO2_{ext} - PO2_{lung}) \times \left[\frac{d}{dt}(vol)\right]_+ - A \times PO2_{lung}\right)$$

$$\frac{d}{dt}(PO2_{blood}) = B \times PO2_{lung} - M \times PO2_{blood}\left(\frac{\Delta nO2_{\text{blood}}}{\Delta PO2_{\text{lung}}}\right)$$

where $r = 0.001$ is the rise/decay time of the motor unit synapse, $[T] = T_{max}/(1+\exp(-(V-V_T)/K_p))$ is the neurotransmitter concentration with $T_{max} = 1$, $V_T = 2$, and $K_p = 5$; $Vol_0 = 2$ is the unloaded lung volume, $E_1 = 0.0025$, $E_2 = 0.4$; $PO2_{ext} = 159.6$ is oxygen in the external air; $A = 6 \times 10^{-5}$ and $B = \times 10^{-5}$ are rates of oxygen transfer from the lungs to the blood, and $M = 7 \times 10^{-5}$ is the rate of metabolic demand for oxygen from the tissues. $[x]_+$ denotes $\max(x, 0)$.

ACKNOWLEDGMENTS

We thank P. Getsy and C. Mayer for assistance with the *in vitro* experiments and F. Orgeta for assistance with RTXI.

References

[1] L F Abbott. Theoretical neuroscience rising. *Neuron*, 60(3):489–95, Nov 2008.

[2] J Best, A Borisyuk, J Rubin, D Terman, and M Wechselberger. The dynamic range of bursting in a model respiratory pacemaker network. *SIAM J Appl Dyn Sys*, 4:1107–1139, 2005.

[3] Robert J. Butera Jr., John Rinzel, and Jeffrey C. Smith. Models of Respiratory Rhythm Generation in the preBötzinger Complex. I. Bursting Pacemaker Neurons. *J Neurophysiol*, 82(1):382–397, 1999.

[4] Robert J. Butera Jr., John Rinzel, and Jeffrey C. Smith. Models of Respiratory Rhythm Generation in the preBötzinger Complex. II. Populations of Coupled Pacemaker Neurons. *J Neurophysiol*, 82(1):398–415, 1999.

[5] Christopher A Del Negro, Naohiro Koshiya, Robert J Butera, Jr, and Jeffrey C Smith. Persistent sodium current, membrane properties and bursting behavior of pre-Bötzinger complex inspiratory neurons *in vitro*. *J Neurophysiol*, 88(5):2242–50, Nov 2002.

[6] Casey O Diekman, Peter J Thomas, and Cristopher G Wilson. Eupnea, tachypnea, and autoresuscitation in a closed-loop respiratory control model. *J Neurophysiol*, 118(4):2194–2215, Oct 2017.

[7] CO Diekman, CG Wilson, and PJ Thomas. Spontaneous autoresuscitation in a model of respiratory control. *Conf Proc IEEE Eng Med Biol Soc*, pages 6669–6672, 2012.

[8] I A Fleidervish and M J Gutnick. Kinetics of slow inactivation of persistent sodium current in layer V neurons of mouse neocortical slices. *J Neurophysiol*, 76(3):2125–30, Sep 1996.

[9] Carlo R. Laing and Ioannis G. Kevrekidis. Periodically-forced finite networks of heterogeneous globally-coupled oscillators: A low-dimensional approach. *Physica D: Nonlinear Phenomena*, 237(2):207 – 215, 2008.

[10] R.J. Lin, J. Bettencourt, J.A. White, D.J. Christini, and R.J. Butera. Real-time Experiment Interface for biological control applications. In *Engineering in Medicine and Biology Society (EMBC), 2010 Annual International Conference of the IEEE*, pages 4160 –4163, 31 2010-sept. 4 2010.

[11] William H Nesse, Alla Borisyuk, and Paul C Bressloff. Fluctuation-driven rhythmogenesis in an excitatory neuronal network with slow adaptation. *J Comput Neurosci*, 25(2):317–33, Oct 2008.

[12] Ryland W Pace, Devin D Mackay, Jack L Feldman, and Christopher A Del Negro. Role of persistent sodium current in mouse preBötzinger Complex neurons and respiratory rhythm generation. *J Physiol*, 580(Pt. 2):485–96, Apr 2007.

[13] Karl R. Popper. *Conjectures and Refutations: The Growth of Scientific Knowledge*. Routledge, 1992 reprinting edition, 1963.

[14] Astrid A Prinz, Cyrus P Billimoria, and Eve Marder. Alternative to hand-tuning conductance-based models: construction and analysis of databases of model neurons. *J Neurophysiol*, 90(6):3998–4015, Dec 2003.

[15] J. Rubin and D. Terman. Synchronized activity and loss of synchrony among heterogeneous conditional oscillators. *SIAM Journal on Applied Dynamical Systems*, 1(1):146–174, 2002.

[16] A.A. Sharp, M.B. O'Neil, L.F. Abbott, and E. Marder. The dynamic clamp: artificial conductances in biological neurons. *Trends Neurosci.*, 16(10):389–94, Oct 1993.

[17] JC Smith, HH Ellenberger, K Ballanyi, DW Richter, and JL Feldman. Pre-Bötzinger complex: a brainstem region that may generate respiratory rhythm in mammals. *Science*, 254(5032):726–729, 1991.

[18] M. Vreugdenhil, C. Hoogland, C. van Veelen, and W. Wadman. Persistent sodium current in subicular neurons isolated from patients with temporal lobe epilepsy. *Eur J Neurosci*, 19:2769–2778, 2004.

[19] S. Wu, Y. Lo, A. Shen, and B. Chen. Contribution of non-inactivating Na^+ current induced by oxidating agents to the firing behavior of neuronal action potentials: experimental and theoretical studies from NG108-15 neuronal cells. *Chinese Journal of Physiology*, 54:19–29, 2011.

[20] H Yu, RR Dhingra, TE Dick, and RF Galán. Effects of ion channel noise on neural circuits: an application to the respiratory pattern generator to investigate breathing variability. *J Neurophysiol*, 117(1):230–242, Jan 2017.